ASTROBIOLOGY
Volume 17, Number 4, 2017

DOI: 10.1089/ast.2016.1488



# Radioresistance of Adenine to Cosmic Rays

Gabriel S. Vignoli Muniz,[1] Christian F. Mejía,[1,2] Rafael Martinez,[1,3] Basile Auge,[1] Hermann Rothard,[1] Alicja Domaracka,[1] and Philippe Boduch[1]

**Abstract**

The presence of nucleobases in carbonaceous meteorites on Earth is an indication of the existence of this class of molecules in outer space. However, space is permeated by ionizing radiation, which can have damaging effects on these molecules. Adenine is a purine nucleobase that amalgamates important biomolecules such as DNA, RNA, and ATP. Adenine has a unique importance in biochemistry and therefore life. The aim of this work was to study the effects of cosmic ray analogues on solid adenine and estimate its survival when exposed to corpuscular radiation.

Adenine films were irradiated at GANIL (Caen, France) and GSI (Darmstadt, Germany) by 820 MeV $Kr^{33+}$, 190 MeV $Ca^{10+}$, 92 MeV $Xe^{23+}$, and 12 MeV $C^{4+}$ ion beams at low temperature. The evolution of adenine molecules under heavy ion irradiation was studied by IR absorption spectroscopy as a function of projectile fluence.

It was found that the adenine destruction cross section ($\sigma_d$) follows an electronic stopping power ($S_e$) power law under the form: $CS_e^n$; $C$ is a constant, and the exponential $n$ is a dimensionless quantity. Using the equation above to fit our results, we determined $\sigma_d = 4 \times 10^{-17}\ S_e^{1.17}$, with $S_e$ in kiloelectronvolts per micrometer (keV $\mu m^{-1}$). New IR absorption bands arise under irradiation of adenine and can be attributed to HCN, $CN^-$, $C_2H_4N_4$, $CH_3CN$, and $(CH_3)_3CNC$.

These findings may help to understand the stability and chemistry related to complex organic molecules in space. The half-life of solid adenine exposed to the simulated interstellar medium cosmic ray flux was estimated as $(10 \pm 8) \times 10^6$ years. Key Words: Heavy ions—Infrared spectroscopy—Astrochemistry—Cosmic rays—Nucleobases—Adenine. Astrobiology 17, 298–308.

## 1. Introduction

Adenine, $C_5H_5N_5$, is the simplest purine nucleobase and the only nucleobase that does not contain oxygen in its composition. It is an integral part of biomolecules of unique importance such as DNA, RNA, and ATP. The adenine molecule is evolutionarily preserved in all living beings, including viruses. Several theories claim that organic complex molecules or their precursors may have reached early Earth via comets and meteorites (Oró, 1961; Chyba and Sagan, 1992). There is evidence that comets and meteorites carry organic molecules such as amino acids and nucleobases or their precursors (Burton *et al.,* 2014; Wright *et al.,* 2015; Altwegg *et al.,* 2016). Those molecules were identified in carbonaceous meteorites on Earth, and the hypothesis that their presence is due to environmental pollution has been discarded, given the amount, structure, and non-terrestrial isotopic composition of these compounds (Shimoyama *et al.,* 1990; Cooper *et al.,* 2001; Martins *et al.,* 2008; Callahan *et al.,* 2011). Moreover, some experiments in the laboratory have shown that the formation of complex organic molecules such as amino acids and nucleobases in astrophysical environments is a possibility (Hörst *et al.,* 2012; Nuevo *et al.,* 2014). The destruction or resistance of adenine in condensed phase has been studied with the use of UV photons (Peeters *et al.,* 2003; Guan *et al.,* 2010), X-rays (Pilling *et al.,* 2011), and electrons (Evans *et al.,* 2011). Furthermore, films of all four nucleobases that form the DNA molecule have been irradiated with $Ar^+$ at low energy (30 keV), and adenine was found to be the least radiosensitive of those four nucleobases (Huang *et al.,* 2014). However, there is no such data about the effects of heavy ions at high energy (cosmic ray analogues).

Several groups have studied irradiation of ices that contain complex organic molecules such as amino acids, nucleobases, and polycyclic aromatic hydrocarbons (de Barros *et al.,* 2012; Gerakines *et al.,* 2012; Cataldo *et al.,* 2013;

[1]Centre de Recherche sur les Ions, les Matériaux et la Photonique, Normandie Univ, ENSICAEN, UNICAEN, CEA, CNRS, CIMAP, Caen, France.
[2]Departamento de Física, Pontifícia Universidade Católica do Rio de Janeiro, Rio de Janeiro, Brazil.
[3]Departamento de Física, Universidade Federal do Amapá, Macapá, Brazil.

Gerakines and Hudson, 2013; Mejía *et al.,* 2013). In the present study, we focused on the effects on adenine due to exposure to galactic cosmic ray analogues. Although less than 1% of galactic cosmic rays consist of heavy ions at high energy, it has been shown that their effects on the destruction and formation of new molecules cannot be neglected (de Barros *et al.,* 2012). With the use of different swift heavy ions, it is possible to determine the destruction cross section of adenine as a function of electronic stopping power. Here, we have evaluated the survival of adenine in the interstellar medium (ISM) and dense clouds (DCs).

## 2. Experimental Methodology

### 2.1. Sample preparation

Adenine powder purchased from Sigma-Aldrich (purity ≥99%) was dissolved in a solution of ethanol and water (Krzaczkowska *et al.,* 2004) (60.8% ethanol in water v/v) at a concentration of 1.0 mg $mL^{-1}$, and the solution was exposed to ultrasound until all solids were visibly dissolved. Thereafter, drops of this solution were dripped directly onto a ZnSe window (13 mm diameter, thickness 2 mm). The window was then heated up to 100°C until the liquid solvent evaporated and, consequently, the solid adenine samples were obtained.

### 2.2. Sample irradiation

Adenine films were irradiated at the beam lines IRRSUD (92 MeV $Xe^{23+}$, 12 MeV $C^{4+}$) and SME (820 MeV $Kr^{33+}$) at GANIL (Caen, France) and at the M-Branch of UNILAC (190 MeV $Ca^{10+}$) at GSI (Darmstadt, Germany).

The experiments at GANIL were performed in the CASIMIR setup (Seperuelo Duarte *et al.,* 2010; Mejía *et al.,* 2015). Each sample was mounted on a cold finger located inside a high-vacuum chamber ($10^{-8}$ mbar). The objective of our setup was to simulate conditions, that is, temperature and pressure, within astronomical environments such as DCs and the ISM. The temperatures within these environments range from 10 to 50 K (Muñoz Caro and Schutte, 2003); thus the samples were irradiated at low temperature (13 K). Unfortunately, it is not possible to create the same pressure range as those that occur in astronomical environments ($10^3$ to $10^6$ atoms $cm^{-3}$) (Muñoz Caro and Schutte, 2003); so the main difficulty with working at low temperatures, under the pressures our setup was capable of generating, was the deposition of the residual gas, notably water and $CO_2$. Nonetheless, in those few hours needed to run our experiment, the condensed ice on our samples was not thick enough to change the regime of deposition of energy of the incoming ions.

As illustrated in Fig. 1, the copper shield (which is used for thermal isolation) was coupled to the cold finger and both turned together. The irradiation was performed at a position of 0°; then at the intermediary fluences the ion beam was switched off and the sample turned to 90° and the IR spectra recorded. To prevent sputtering, one of the samples was turned to 180° and covered with a thin water-ice layer (0.22 μm) before irradiation began.

The IR absorption spectra were obtained *in situ* before and after irradiation with a Fourier transform infrared (FTIR) spectrometer [Nicolet Magna 550, mercury-cadmium-telluride detector cooled with liquid nitrogen], operating in transmission

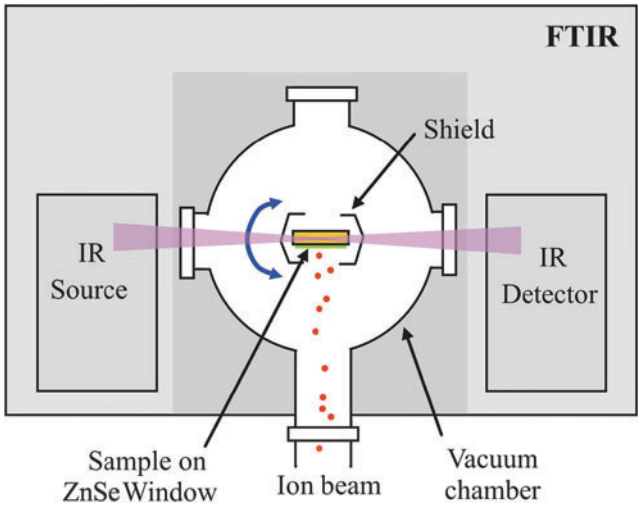


**FIG. 1.** Schematic experimental setup employed for bombardment of solid adenine by heavy ions (Seperuelo Duarte *et al.,* 2010).

mode. The spectra were acquired by 128 scans in the wavenumber range from 4000 $cm^{-1}$ to 700 $cm^{-1}$ with a resolution of 1 $cm^{-1}$. Note that the background of the ZnSe window was taken before the irradiation at 300 and 13 K to avoid thermal optical effects.

The average flux was $10^9$ ions $cm^{-2}$ $s^{-1}$. Using the Stopping and Ranges of Ions in Matter (SRIM) software (Ziegler *et al.* 2012), we calculated the electronic ($S_e$) and nuclear energy loss ($S_n$) of the ions in pure adenine and adenine covered with water ice. The projectile and target properties are summarized in Table 1.

The experimental setup at GSI was similar, though the irradiation temperature was slightly higher (≈20 K) (see Severin *et al.,* 2008; Mejía *et al.,* 2015).

### 2.3. Infrared absorption spectrum of adenine: band identification

The adenine molecule (Fig. 2) is formed by two heterocyclic rings, one with six atoms (R6) and the other with five atoms (R5). Its empirical formula is $C_5H_5N_5$. It has a molecular weight equal to 135.13 g $mol^{-1}$, and the adenine film density adopted was 1.5 g $cm^{-3}$ (Evans *et al.,* 2011).

The present adenine IR absorption spectrum at room temperature (peak position and assignment) is in good agreement with the results of other authors (Mohamed *et al.,* 2009; Saïagh *et al.,* 2014). Table 2 presents the comparison between the present work and the work of the cited authors.

Figure 3 shows the comparison of the adenine spectra at room temperature and at 13 K. The spectrum of solid adenine at 13 K exhibits a new absorption band at 3260 $cm^{-1}$ and a small shift to higher wavenumbers. The band at 3115 $cm^{-1}$ becomes thinner, and the absorption peak in the alpha band is better resolved.

### 2.4. Sample thickness

Saïagh *et al.* (2014) referred to the large absorption region in the adenine spectrum between 3400 and 2000 $cm^{-1}$ as ''alpha band.'' By using different methods such as laser

Table 1. Summary of the Experimental Parameters

| *Ion beam* | *Energy (MeV)* | *Electronic stopping power ($10^3$ keV μm$^{-1}$)* | *Nuclear stopping power (keV μm$^{-1}$)* | *Adenine film thickness (μm)* | *Water-ice thickness (μm)* | *Penetration depth (μm)* |
|---|---|---|---|---|---|---|
| $Xe^{23+}$ | 92 | 11.2 | 71 | 0.29 | 0 | 16 |
| $Kr^{33+}$ | 820 | 5.8 | 3.6 | 0.45 | 0 | 120 |
| $Ca^{10+}$ | 190 | 3.1 | 2.2 | 0.22 | 0 | 51 |
| $Ca^{10+}$ | 190 | 3.1 | 2.2 | 0.25 | 0.22 | 51 |
| $C^{4+}$ | 12 | 1.0 | 0.9 | 0.09 | 0 | 12 |
| $C^{4+}$ | 12 | 1.0 | 0.9 | 0.28 | 0 | 12 |

interference and interferometric microscopy, it has been shown that there is a linear relation between the thickness of solid adenine and its alpha band absorption at room temperature (Saïagh *et al.,* 2014). In the present work, adenine IR spectra were first recorded at room temperature, and the thickness of the samples was estimated by using the linear relationship. Then, the sample was cooled down to around 20 K as earlier discussed in Section 2.2. Table 1 summarizes the experimental parameters.

## 3. Results

### 3.1. Adenine fragmentation

During energetic heavy ion irradiation of the adenine film, its overall IR absorption intensity decreases (Fig. 4). Furthermore, new IR absorption bands clearly arise between 2300 and 2000 cm$^{-1}$. According to the Beer-Lambert law, the absorption area is directly proportional to the column density (number of molecules per cm$^2$). Therefore, the reduction of IR absorption area is due to adenine molecule disappearance caused by either destruction or sputtering. Both effects (destruction and sputtering) can be quantified by introduction of the ''apparent destruction cross section'' ($\sigma_d$) (de Barros *et al.,* 2012; Mejía *et al.,* 2013). The evolution of the peak area as a function of the ion fluence can be written as

$$A = A_0 e^{-\sigma_d F} \quad (1)$$

where $F$ is the fluence, $A_0$ is the initial absorption of a given peak area, and $\sigma_d$ is the apparent destruction cross section.

The intensity of certain bands decreases more rapidly than that of others, yielding different values of the apparent destruction cross section (Appendix Table A1). Effectively, the destruction cross section for a molecule corresponds to the highest value. However, some authors prefer to work with ''average'' cross sections (Peeters *et al.,* 2003; Evans *et al.,* 2011; Portugal *et al.,* 2014). Here, we choose the cross section that corresponds to the dissociation of NCN at R5 (914 cm$^{-1}$), because not only does it show one of the highest observed values, but also the band located at 914 cm$^{-1}$ is not overlapped by water-ice IR absorption bands and thus can be analyzed in a straightforward way without deconvolution. In the case of the samples covered by water ice, only the absorption peak area located at 914 cm$^{-1}$ was taken into consideration.

Figure 5 shows the evolution of the peak area at 914 cm$^{-1}$ of pure adenine and adenine covered with water ice as a function of (190 MeV) $Ca^{10+}$ fluence. Water ice on adenine film prevents the sputtering. The difference between the two curves is within the error bar, showing that the evolution of adenine under irradiation is dominated by radiolysis. Moreover, since the difference between the two curves is insignificant, it is not possible to determine the adenine sputtering yield per incoming ion.

The physicochemical molecular modification induced by corpuscular irradiation can be divided into direct and indirect effects. The projectiles ionize the target directly; in the present case, ionization of adenine rings followed by dissociation or even atomization of the entire molecule occurs. The indirect effects are related to ionization of neighboring molecules (*e.g.,* if the molecule is embedded in a matrix of water), which produces free radicals that can diffuse and interact with adenine and provoke its rupture.

According to Pullman and Pullman (1963), the reaction with free radicals and nucleobases consists of the addition of a pair of free radicals to one of the double bonds of the nucleobase. In the case of adenine, the most probable site of interaction with free radicals is the bond between the $N_7$-$C_8$ at R5. This is due to a high free valence of the atoms in this bond, in this case the free valence of the $C_8$. Note that the absorption band at 914 cm$^{-1}$ corresponds to the vibration of NCN at R5; this is an indication that the interaction between free radicals and adenine is important for its radiosensibility.

Table 3 displays the apparent cross section (914 cm$^{-1}$) and the average apparent cross section for different projectiles.

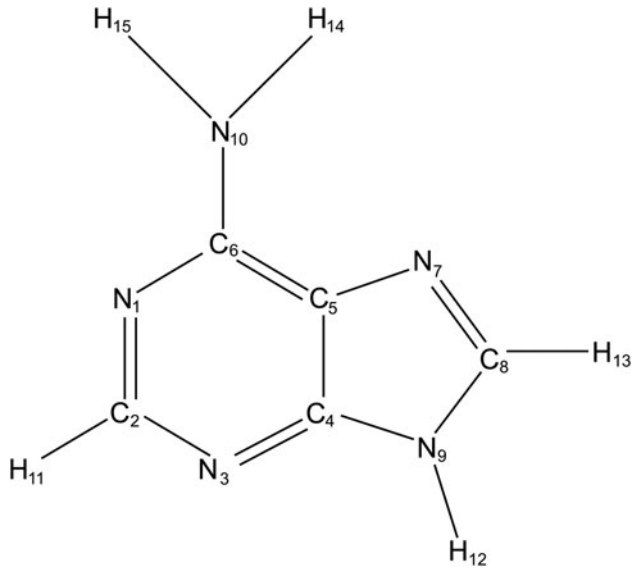


**FIG. 2.** The structure of the adenine molecule (schematic).

Table 2. Band Assignment for Solid Adenine

| $\nu_i$ | *Assignment* | *Definition* | *Mohamed* et al. *(2009)* | *Saïagh* et al. *(2014)* | *Present work* |
|---|---|---|---|---|---|
| $\nu_1$ | $NH_2$ | anti-symmetric stretch | 3426vw | | |
| $\nu_2$ | $N_9H$ | Stretch | 3347sh | | 3347 |
| $\nu_3$ | $NH_2$ | symmetric stretch | 3296s | 3314 | 3293 |
| $\nu_4$ | $C_8H$ | Stretch | 3119vs | 3122 | 3115 |
| | | | 2980 | 2984 | 2975 |
| | | | | 2798 | 2790 |
| | | | | 2689 | 2685 |
| $\nu_5$ | $C_2H$ | Stretch | 2980s | 2984 | 2975 |
| $\nu_6$ | $NH_2$ | deformation (scissors) | 1673vs | 1665 | 1668 |
| $\nu_7$ | CN R(6) | ring stretch | 1603vs | 1600 | 1600 |
| $\nu_8$ | CC R(6) | ring stretch | 1603vs | 1600 | 1600 |
| $\nu_9$ | CN R(5) | ring stretch | 1506sh | | 1508 |
| $\nu_{10}$ | CN R(6) | ring stretch | 1483sh | | |
| $\nu_{11}$ | CC R(6) | ring stretch | 1451m | | 1451 |
| $\nu_{12}$ | $C_2H$ | in-plane deformation | 1420s | 1417 | 1418 |
| $\nu_{13}$ | $C_6N_{10}$ | Stretch | 1368w | 1366 | 1367 |
| $\nu_{14}$ | CN R(5) | ring stretch | 1335s | 1330 | 1332 |
| $\nu_{15}$ | CN R(6) | ring stretch | 1309s | 1307 | 1308 |
| $\nu_{16}$ | $C_8H$ | in-plane deformation | 1252s | 1251 | 1252 |
| $\nu_{17}$ | CN R(5) | ring stretch | 1252s | 1251 | 1252 |
| $\nu_{18}$ | CN R(5) | ring stretch | 1126m | 1120 | 1126 |
| $\nu_{19}$ | $N_9H$ | in-plane deformation | 1065sh | | |
| $\nu_{20}$ | $NH_2$ | Rock | 1025m | 1023 | 1022 |
| $\nu_{21}$ | $C_2H$ | Wagging | 939s | | 939 |
| $\nu_{22}$ | NCN R(5) | ring deformation | 913s | | 911 |
| $\nu_{23}$ | NCN R(6) | ring deformation | 872sh | | 874 |
| $\nu_{24}$ | $C_8H$ | Wagging | 846sh | | 847 |
| $\nu_{25}$ | R(6) | ring torsion | 797w | | 797 |
| $\nu_{26}$ | R(6) breath | ring breathing | 723m | | 723 |

Comparison between our results and those of Mohamed *et al.* (2009) and Saïagh *et al.* (2014).

These values are around $10^4$ times higher than for 5 keV electrons (Evans *et al.,* 2011), $10^9$ times higher than for UV photons (Guan *et al.,* 2010), $10^5$ times higher than for X-rays (Pilling *et al.,* 2011), and $10^6$ times higher than for UV photon degradation of adenine in argon matrix (more details in Section 3.2). The typical range of cross sections can be seen in Appendix Table A1 for the following: (1) $Xe^{23+}$ (92 MeV) in the order of magnitude of $10^{-12}$ $cm^2$; (2) $Kr^{33+}$ (820 MeV) between $10^{-12}$ and $10^{-13}$ $cm^2$; (3) $Ca^{10+}$ (190 MeV) $10^{-13}$ $cm^2$; and (4) $C^{4+}$ (12 MeV) between $10^{-13}$ and $10^{-14}$ $cm^2$.

Figure 6 shows the apparent destruction cross section as a function of the electronic stopping power ($S_e$). Several

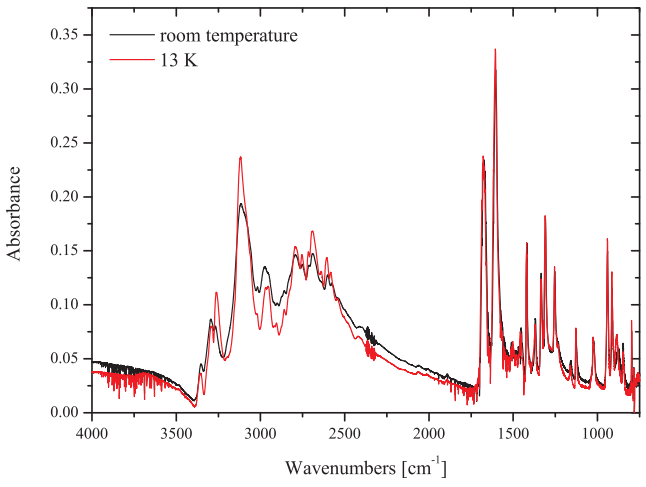


**FIG. 3.** Infrared absorption spectra of solid adenine at 13 and 300 K.

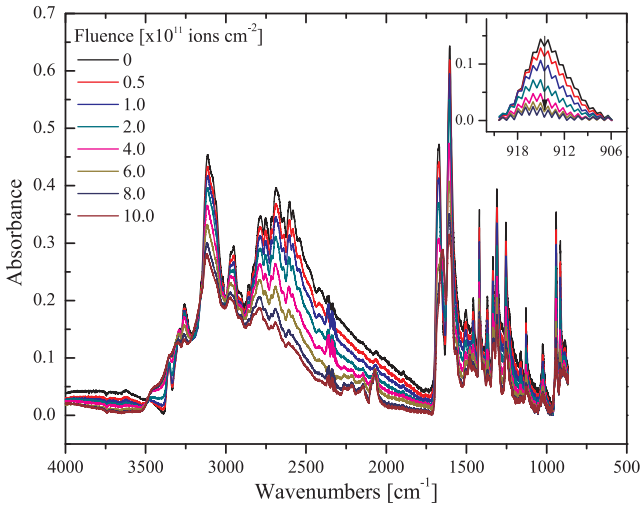


**FIG. 4.** Infrared absorption spectra of adenine at 13 K under irradiation of (92 MeV) $Xe^{23+}$ at different fluences. Inset: Infrared absorption peaks at 914 $cm^{-1}$ at different ion fluences.

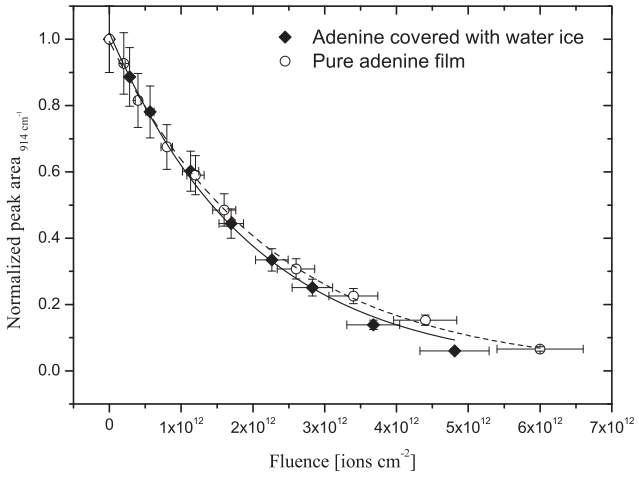


**FIG. 5.** Evolution of peak areas at 914 $cm^{-1}$ of pure adenine film and adenine film covered with water ice as a function of fluence of (190 MeV) $Ca^{10+}$.

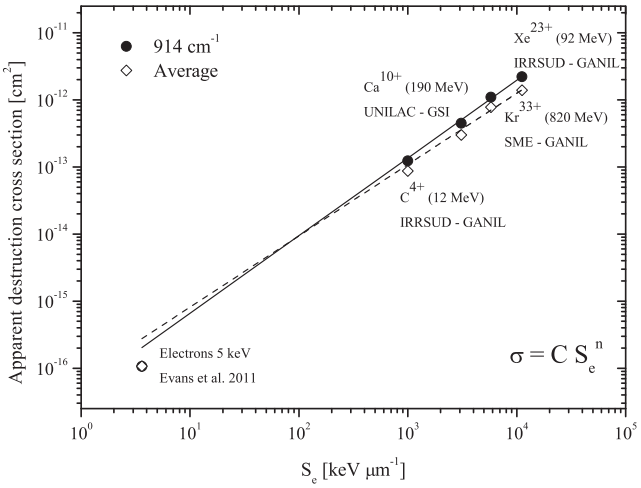


**FIG. 6.** Adenine destruction cross section (914 $cm^{-1}$) and the average destruction cross section as a function of the electronic stopping power.

authors have observed that the destruction cross section obeys a power law: $\sigma = CS_e^n$ (de Barros *et al.,* 2011, 2014; Andrade *et al.,* 2013; Dartois *et al.,* 2013; Mejía *et al.,* 2013). Using this equation to fit the experimental data as a function of the electronic stopping power, calculated with SRIM (Ziegler *et al.,* 2012), we find $\sigma = 4 \times 10^{-17} S_e^{1.17}$, with $S_e$ in kiloelectronvolts per micrometer (keV $\mu m^{-1}$). These experiments were performed at two different laboratories (GANIL and GSI). Note that the adenine destruction cross sections obtained at those two different accelerators and with two different experimental setups fall onto one curve; this shows a good consistency and reproducibility of our experiments. Moreover, adenine destruction cross sections for electrons at 5 keV (Evans *et al.,* 2011) match with our curve. The average destruction cross section is close to our curve, with $n = 1.08$.

### 3.2. Formation of new molecules

After a deposited local dose higher than 1 eV/molecule, all samples started to exhibit a new absorption band between 2300 and 2050 $cm^{-1}$. Moreover, vibration modes of C═N (1654, 1478, and 800 $cm^{-1}$) were observed. Those vibration modes are expected for a primary amine (Günzler and Gremlich, 2002) and are correlated to the opening of the adenine rings. To analyze the formation of new molecules, we deconvoluted the large band (2300–2050 $cm^{-1}$) that appears when adenine is irradiated by $Xe^{23+}$ at high fluence ($1 \times 10^{12}$ ions $cm^{-2}$) as shown in Fig. 7. This region is characteristic of C≡N and C≡C absorption, which is observable through the deconvolution of absorptions at 2044, 2070, 2092, 2100, 2124, 2144, 2174, 2212, 2240, and 2262 $cm^{-1}$.

Since the adenine IR absorption spectrum is complex, it is difficult to identify new molecular species formed by the fragmentation of these nucleobases, and it is probable that new absorption bands overlap with the bands from residual adenine.

Nevertheless, it is possible to speculate on some candidates of new molecular species responsible for observed absorption. Some molecules are natural candidates, such as HCN (2100 $cm^{-1}$) (Moore and Hudson, 2003; Burgdorf *et al.,* 2010), CN (2090 $cm^{-1}$) (Moore and Hudson, 2003), and $C_2H_4N_4$ (2212 and 2174 $cm^{-1}$) (Gerakines *et al.,* 2004). The molecule $(CH_3)_3CNC$, which has an absorption peak at 2140 $cm^{-1}$ (Hudson and Moore, 2004), makes it yet another

TABLE 3. THE APPARENT DESTRUCTION CROSS SECTIONS OF ADENINE AND THE AVERAGE DESTRUCTION CROSS SECTION OF ADENINE FOR DIFFERENT PROJECTILES

| *Projectile* | *Apparent destruction cross section* ($\times 10^{-13}$ $cm^2$) | *Average apparent destruction cross section* ($\times 10^{-13}$ $cm^2$) |
|---|---|---|
| $Xe^{23+}$ | 22.2 ± 0.3 | 14 ± 1 |
| $Kr^{33+}$ | 10.9 ± 0.2 | 7.8 ± 0.9 |
| $Ca^{10+}$ | 4.5 ± 0.4 | 3.0 ± 0.8 |
| $C^{4+}$ | 1.24 ± 0.06 | 0.87 ± 0.02 |

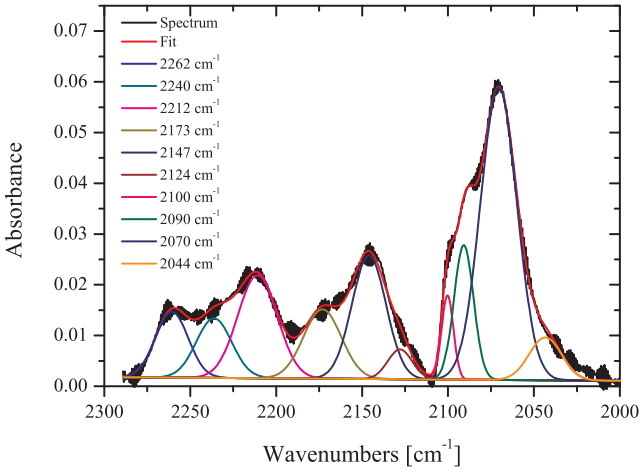


**FIG. 7.** Deconvolution of the band between 2300 and 2000 $cm^{-1}$ of adenine film irradiated with (92 MeV) $Xe^{23+}$ at fluence of $1.0 \times 10^{12}$ ions $cm^{-2}$.

promising candidate. Its full width at half maximum (FWHM) of this absorption peak is 26.4 $cm^{-1}$. Hence, we can disregard CO as a candidate because even with the same absorption peak at 2140 $cm^{-1}$ as $(CH_3)_3CNC$, its FWHM peak at 1.6 $cm^{-1}$ is too small for it to be CO (van Broekhuizen *et al.,* 2006). The IR absorption band located at 2240 $cm^{-1}$ is certainly made by a nitrile that has absorption peaks close within that region (Hudson and Moore, 2004; Evans *et al.,* 2011). However, the interaction between the molecules in their neighborhood can shift the IR absorption peaks and make it difficult to determine which molecule is truly responsible for this absorption. The absorption peak at around 2260 $cm^{-1}$ is the typical vibration of C≡N; for example, some molecules and radicals like HCNO (Peeters *et al.,* 2003) and cyanomethyl radical ($CH_2$−C≡N) (Pilling *et al.,* 2012) have this absorption band. It is important to mention here that, despite the absence of oxygen in an adenine molecule, pollution from residual gases like water and $CO_2$ is not excluded; therefore, formation of molecules containing oxygen cannot be eliminated. We were unable to attribute any candidates to the absorption peaks at 2044 or 2070 $cm^{-1}$. There is also a probability of the formation of $N_2$, but these symmetric molecules are difficult to detect by FTIR.

Exposing solid adenine to electromagnetic ionizing radiation did not produce new IR absorption bands. Guan *et al.* (2010) and Pilling *et al.* (2011) obtained just 2% of photolyzed adenine. Probably, the number of new molecules generated by the adenine photodegradation is under the limit of detection by IR absorption spectroscopy. In fact, in our case we only observe new IR absorption bands after the degradation of at least 20% of initial adenine. Poch *et al.* (2014) also exposed thin films of complex organic molecules to UV radiation. Among those molecules adenine was also photolyzed for a long time (2.5 days). Their results are in agreement with ours; for example, they observed a new IR absorption band that emerged from the adenine radiolysis. They assigned those absorption peaks to the vibration of isonitrile groups (R-N≡C) and/or nitrile groups (R-C≡N), the stretching of C=C and C=N corresponding to a vibration of a primary amine. Furthermore, they observed an absorption peak at 2173 $cm^{-1}$; we believe that this absorption peak also could be attributed to $C_2H_4N_4$ as in the case of our experiments. Moreover, note that one more indication of the absence of new absorption peaks in the experiments of Guan *et al.* (2010) and Pilling *et al.* (2011) is a low susceptibility of adenine to UV photons (Table 4). The photon fluence used by Poch *et al.* (2014) was around 1 order of magnitude higher than that used by Guan *et al.* (2010) and 4 orders of magnitude higher than that used by Pilling *et al.* (2011).

The adenine fragmentation by 5 keV electrons (Evans *et al.,* 2011) produced an absorption band at 2235 $cm^{-1}$, assigned as R−C≡N. With heavy ions, we also observed the emergence of this band after irradiation (2240 $cm^{-1}$). The formation of HCN or $CN^-$ was not detected by Evans *et al.* (2011). Their samples were covered with thin $O_2$ ice. Indeed, they describe new bands at 2108, 1035, 702 ($O_3$), 1871 (R−C=O), 1750 (R−C=O), 1610 (C−O−C), 1242 (C−O−C), and 737 (C−O−C) $cm^{-1}$. In our work, these bands were not observed. The difference between our observations and those of Evans *et al.* (2011) are probably caused by the reactions with $O_2$ ice layers in their samples.

## 4. Discussion

### 4.1. Comparison between different sources of radiation

The comparison of molecular radiation damage provoked by different radiation sources needs to be analyzed with attention because electromagnetic and corpuscular radiation have different energy loss mechanisms. Moreover, the physical state and the environment of the irradiated molecule are important factors for its survival. Guan *et al.* (2010) exposed adenine films to 10.2 eV photons in the laboratory. Using the BIOPAN 6 facility, which was set outside the automated Russian science satellite Foton M3, they also exposed adenine films directly to the solar winds of Earth's orbit. They reported an adenine half-life $10^3$ times higher than that of adenine in an argon matrix exposed to 10.2 eV photons (Peeters *et al.,* 2003). Guan *et al.* (2010) claimed that this difference is due to the adenine's physical state; in an argon matrix, the Van der Walls force and H bonding would be weaker, which would favor molecule fragmentation.

We now compare the effects of different sources of radiation on solid adenine. As discussed by Loeffler *et al.* (2005), the radiation yield $G$ is a useful scaling factor with which to compare effects from different ionizing radiation such as corpuscular and electromagnetic radiation. The definition of $G$ for 10.2 eV photons and corpuscular radiation can be found in their work. To estimate the adenine destruction cross section and the $G$ value for photons of 10.2 eV, we used the results of Guan *et al.* (2010) and Saïagh *et al.* (2014). Table 4 shows the destruction cross section and radiation $G$ yield for various charged projectiles and electromagnetic radiation. The radiation $G$ yield in the

Table 4. The Radiation Yield $G$ and the Destruction Cross Section for Solid Adenine Irradiated by Different Projectiles at Different Energies

| *Projectile* | *Radiation yield* G ($eV^{-1}$) | *Apparent destruction cross section* ($cm^2$) | *Reference* |
|---|---|---|---|
| $Xe^{23+}$ (92 MeV) | 13.13 | $(2.2\pm0.3)\times10^{-12}$ | This work |
| $Kr^{33+}$ (820 MeV) | 12.56 | $(1.1\pm0.2)\times10^{-12}$ | This work |
| $Ca^{10+}$ (192 MeV) | 9.70 | $(4.5\pm0.4)\times10^{-13}$ | This work |
| $C^{4+}$ (12 MeV) | 8.29 | $(1.24\pm0.06)\times10^{-13}$ | This work |
| Electrons (5 keV) | 1.98 | $(1.07\pm0.24)\times10^{-16}$ | Evans *et al.,* 2011 |
| UV photons (10.2 eV) | $4.9\times10^{-5}$ | $(5\pm2)\times10^{-22}$ | Guan *et al.,* 2010; Saïagh *et al.,* 2014 |
| X-rays (150 eV) | — | $3\times10^{-19}$ | Pilling *et al.,* 2011 |

present case is defined as the number of adenine molecules destroyed per 100 eV absorbed. Note that the effect of swift heavy ions is 10 times higher than that of 5 keV electrons and around $10^5$ times higher than that of 10.2 eV photons. This finding clearly shows that, even with low abundance, heavy ions play an important role in the survival of adenine. It was not possible to calculate the radiation $G$ yield for solid adenine irradiated with 150 eV photons because its absorption cross section is unknown. Moreover, the irradiation of adenine by soft X-rays (Pilling *et al.,* 2011) and UV photons (Guan *et al.,* 2010) was performed at room temperature, and the radiation damage depends on temperature (Fryer *et al.,* 1992; Portugal *et al.,* 2014).

Evans *et al.* (2011) estimated the destruction cross section for 1 MeV and 1 keV protons under the assumption that they can be obtained by scaling the 5 keV electron data by the stopping power ratio. We can also estimate the destruction cross section for protons using our findings (Fig. 6). Calculating the electronic stopping power of protons by using the SRIM code (Ziegler *et al.,* 2012) together with the observed power law allows us to estimate the destruction cross section for protons at those energies (1 MeV and 1 keV). We obtain the values $\sigma = 1.5 \times 10^{-15}$ and $\sigma = 2.6 \times 10^{-15}$ cm$^2$ for 1 keV and 1 MeV protons, respectively. The cross sections reported by Evans *et al.* (2011) are 40% lower. However, this approximation is of the same order of magnitude as our calculation, which shows the validity of their extrapolation. It is important to say that the observed power law is valid in the electronic stopping power domain. In the case of 1 MeV and 1 keV protons, the electronic stopping power is at least 1 order of magnitude higher than the nuclear stopping power.

Our findings also allow us to compare the radiosensibility of adenine with the radiosensibility of other organic molecules. Portugal *et al.* (2014) performed an irradiation of glycine with $Ni^{11+}$ (46 MeV) beams at different temperatures (14 and 300 K). Using the SRIM code (Ziegler *et al.* 2012) to estimate the electronic stopping power of adenine for $Ni^{11+}$ (46 MeV), we estimate an adenine destruction cross section of $\sigma = 1.16 \times 10^{-12}$ cm$^2$ for this projectile. This is half the value reported for glycine at 14 K (Portugal *et al.,* 2014). This demonstrates that adenine is less radiosensitive to radiation than glycine, a finding that can probably be explained in terms of aromaticity. Adenine is an aromatic molecule, and it is well known that aromatic molecules are more radioresistant than aliphatic molecules (Pullman and Pullman, 1963; Sawyer *et al.,* 2008). The delocalization of the electrons allows the absorbed energy to spread out in the aromatic rings and prevents bonds between two individual atoms to be broken. In non-aromatic molecules, the absorbed energy is confined to the bonds that make the dissociation more probable.

### 4.2. Astrophysical implications

Radio spectroscopy is currently the most precise technique with which to detect molecules in outer space. However, there is a limitation to the detection of molecules in their solid phase. Despite some theoretical predictions, adenine was not detected in gas phase in space. It has been suggested that formation of adenine can occur inside or on the surface of the interstellar grains (Evans *et al.,* 2011; Chakrabarti *et al.,* 2015), and the presence of complex organic molecules including nucleobases in carbonaceous meteorites (Martins *et al.,* 2008; Callahan *et al.,* 2011) is an indication of abiotic synthesis of those molecules in astrophysical environments.

Therefore, if adenine exists in the ISM, its evolution probably happens inside and/or on the surface of icy grains in DCs. Our experiments are close to this scenario: condensed phase at low temperature. However, in icy grains the complex organic molecules are in a matrix of different elements, notably water. Gerakines and Hudson (2013) reported that organic molecules in water matrix (at different ratios) have distinct radiosensibility; when glycine is embedded in a water matrix, the radiation $G$ yield is 1 order of magnitude smaller. Furthermore, astrochemical processes in space are far from being trivial. In this work, we do not take into account reactions that can happen on the surface of grains. Hence, it is important to mention that the present study is a first attempt to understand adenine radiolysis and an extrapolation to astrophysical environments.

By using the observed power law (Section 3.1) and the SRIM code (Ziegler *et al.,* 2012), it is possible to determine the destruction cross section for the 10 most abundant ions in galactic cosmic rays at different energies. Figure 8 shows the adenine destruction cross section as a function of energy. To estimate the adenine half-life ($\tau_{1/2}$) in the ISM, the same method used by Portugal *et al.* (2014) was applied in Eq. 2:

$$\tau_{1/2} = \ln 2 \left( 4\pi \sum_Z \int_{10^{-1}}^{10^3} \sigma(Z,E)\Phi(Z,E)dE \right)^{-1} \qquad (2)$$

$\sigma(Z, E)$ is the adenine destruction cross section, and $\Phi(Z, E)$ is the differential flux of cosmic ray ions of atomic number $Z$ (the summation was obtained by using the 10 most abundant ions in galactic cosmic rays).

The distribution of cosmic rays is well known at energies above 1 GeV per nucleon (GeV/n) (Webber and Yushak, 1983; Shen *et al.,* 2004). However, particles at low energies can be expelled from the heliosphere by solar wind and

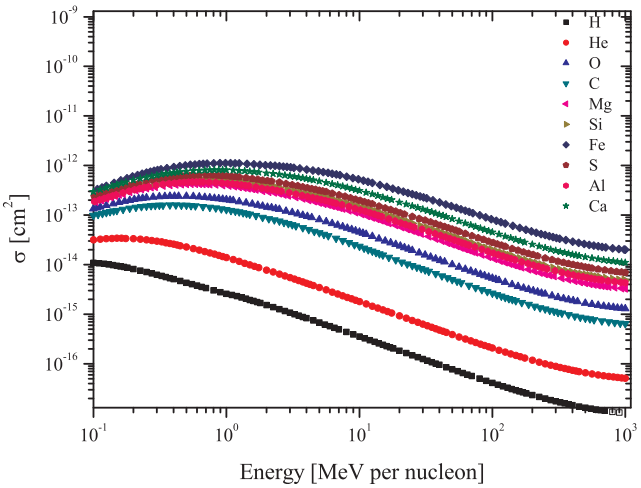


**FIG. 8.** Adenine destruction cross section for different ions as a function of energy.

planetary magnetic fields. The spectra of cosmic rays observed from Earth are therefore modulated; hence the flux of cosmic rays is full of uncertainties, especially at low energies due to this modulation (Shen *et al.,* 2004; Padovani and Galli, 2013). Webber and Yushak (1983) showed that Eq. 3 well represents a simulation of the observable cosmic ray distribution.

$$\Phi(E,Z) = \frac{C(Z)E^{0.3}}{(E+E_0)^3} \tag{3}$$

$C(Z)$ is a normalization constant. The numerical values of the constant $C(Z)$ can be found in the work of Portugal *et al.* (2014). $E_0$ is a parameter that modifies the flux at low energy but does not have an impact at high energies. According to Shen *et al.* (2004), $E_0 = 400$ MeV per nucleon (MeV/n) is the most accurate value to simulate the observed cosmic ray flux. Although Eq. 3 is just an estimation of the flux of cosmic rays, Dartois *et al*. (2013) showed that, with different values of the parameter $E_0$ (200, 400, and 600 MeV/n), it is possible to evaluate cosmic ray ionization rates, which are in agreement with astronomical observations (Indriolo *et al.,* 2007). Following this procedure, we adopted different values of the parameter $E_0$ (200, 400, and 600 MeV/n) to understand the survival of adenine exposed to cosmic rays.

The destruction rate, that is, the product of the destruction cross section and the flux of cosmic rays, will determine the survival of adenine exposed to cosmic rays (Eq. 2). Cosmic rays are ions with a broad energy range from a few megaelectronvolts per nucleon to teraelectronvolts per nucleon. The energy range adopted in this study is from $10^{-1}$ to $10^3$ MeV/n because it is the range with the most intense cosmic ray flux, as it is also within the range that $S_e$ is in, which is at least 2 orders of magnitude higher than $S_n$. Our power law (Fig. 6) is valid in the electronic stopping power regime only. As an example, we plotted (Fig. 9) the loss of energy per unit of path length of iron nuclei in solid adenine as a function of energy; in Fig. 9 both electronic ($S_e$) and nuclear

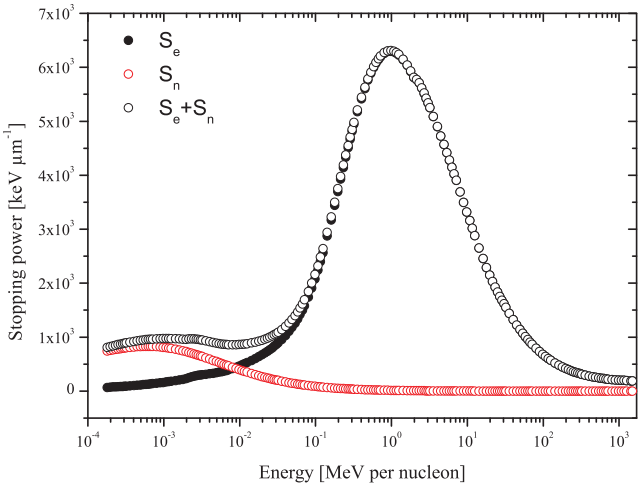


**FIG. 9.** Electronic stopping power ($S_e$), nuclear stopping power ($S_n$), and the total stopping power ($S_e + S_n$) as a function of the projectile energy in solid adenine.

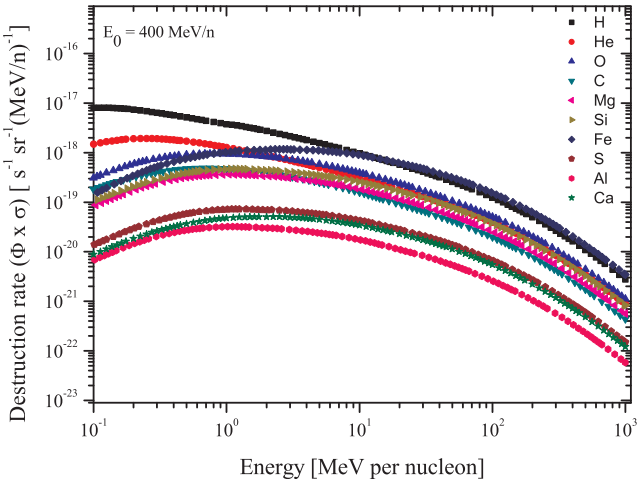


**FIG. 10.** Adenine destruction rate for different ions as a function of energy. $E_0 = 400$ MeV/n.

($S_n$) stopping power are included. It should be kept in mind that maximum energy deposition occurs between 0.1 and 10 MeV/n. Thus, the ion beams employed in this work are good analogues for cosmic rays. Set aside from that, ions with energies above 1 GeV/n deposit a very little amount of energy electronically. There is also the possibility of nuclear reactions.

Figure 10 shows the destruction rate ($\sigma_d \times \Phi$) as a function of energy for different ions. As can be seen in the figure, iron and protons are the biggest contributors to adenine destruction despite the fact that the flux of iron is much smaller than that of protons. This shows the importance of heavy ions: even if less abundant, their contribution cannot be neglected. Table 5 displays the half-life of solid adenine exposed to cosmic rays for different values of $E_0$ in the ISM and the average adenine half-life (the error given is the standard deviation).

As discussed by Peeters *et al.* (2003), the half-life of adenine is different within distinct regions of outer space due to UV deterioration. The scattering provoked by the grains and dust within DCs shields their interior against UV photons emitted from neighboring stars. The secondary UV radiation induced by the impact of cosmic rays on hydrogen plays an important role in those regions, but its flux is 5 orders of magnitude smaller in comparison with UV flux in the diffuse interstellar medium (DISM) (Ehrenfreund *et al.,* 2001; Moore *et al.,* 2001; Palumbo *et al.,* 2008). By using the results of Peeters *et al.* (2003) together with the UV destruction cross section of solid adenine we calculated by

TABLE 5. THE HALF-LIFE OF SOLID ADENINE EXPOSED TO COSMIC RAYS FOR DIFFERENT VALUES OF THE PARAMETER $E_0$ AND THE AVERAGE ADENINE HALF-LIFE

| $E_0$ *(MeV/n)* | *Half-life* $\tau_{1/2}$ *(million years)* |
|---|---|
| 200 | 1.40 |
| 400 | 7.96 |
| 600 | 22.2 |
| Average adenine half-life (million years) | $10 \pm 8$ |

referring to the work of Guan *et al.* (2010), it is possible to estimate the half-life of solid adenine exposed to UV photons in the DISM and DCs: $\tau_{1/2} = 4.5 \times 10^5$ and $\tau_{1/2} = 4.5 \times 10^{10}$ years, respectively. The attenuation of the cosmic rays made by the diffuse gas in the DISM is negligible; even in DCs the cosmic ray flux attenuation is only of the order of 10 times smaller than in the ISM (Ehrenfreund *et al.,* 2001). Therefore, the evolution of adenine in the DISM would be dominated by UV radiation, while inside the DCs it would be dominated by corpuscular radiation. These findings are in agreement with the results of Evans *et al.* (2011). The average time of survival of a DC is around 10 million years (Ehrenfreund *et al.,* 2001). This is indeed close to the order of magnitude of the half-life of adenine evaluated in this work. Our findings suggest that, if adenine was once formed in DCs, it could be possible that those molecules still remain today.

## 5. Conclusion and Outlook

In the present work, the destruction of pure adenine by heavy ions in the electronic stopping power domain was studied. The destruction cross section was determined as a function of electronic stopping power in the form $CS_e^n$, with $n = (1.17 \pm 0.06)$.

Our results exhibit an adenine destruction cross section about $10^9$ times higher than for UV photons, $10^5$ times higher than for soft X-rays, and $10^3$ times higher than for 5 keV electrons. The yield $G$ is around 1 order of magnitude higher for heavy ions in comparison with 5 keV electrons and $10^5$ times higher than for UV photons. Our results show that destruction of adenine exposed to cosmic rays is dominated by iron nuclei and hydrogen. This is necessary for an understanding of formation and, in particular, survival of nucleobases in outer space.

Moreover, the adenine half-life was estimated inside DCs as $\tau_{1/2} = (10 \pm 8)$ million years, which means there is the possibility of still finding remnants in those regions.

New IR absorption bands that come from the degradation of adenine under irradiation were detected. Molecules such as HCN, $CN^-$, and $C_2H_4N_4$ are possible candidates for these absorption bands. The present results can be of help toward the understanding of the abundance and origin of those organic molecules.

## Acknowledgments

This work was supported by Brazilian agencies CNPq (INEspaço and Science without Borders) and FAPERJ, as well as the CAPES-COFECUB French-Brazilian exchange program. It is a pleasure to thank Thierry Been, Jean-Marc Ramillon, Toiammou Madi, Dr. Florent Moisy, and Dr. Clara Grygiel for their invaluable support. Many thanks to Dr. Emmanuel Balanzat, Dr. Yvette Ngono-Ravache, Prof. Dr. Enio da Silveira, and Dr. Diana Andrade for important discussions. The authors wish to acknowledge the staff of GANIL and GSI for their invaluable help during the course of the experiments. We are particularly thankful to Prof. Dr. Christina Trautmann, Dr. Daniel Severin, Dr. Markus Bender, Alexander Warth, and Arne Siegmund at GSI. The experiments were performed at *Grand Accélérateur d'Ions Lourds* (GANIL) Caen, France, and at GSI *Helmholtzzentrum für Schwerionenforschung,* Darmstadt, Germany. Part of this work was supported by the ANR IGLIAS project, grant ANR-13-BS05-0004 of the French *Agence Nationale de la Recherche*. This work was co-funded by the European Commission, FP7 for RTD Capacities Program (Contract No. 262010, ENSAR), and the EU's Horizon 2020 Research and Innovation Programme (grant agreement No. 654002 ENSAR2).

## Author Disclosure Statement

No competing financial interests exist.

## References

Altwegg, K., Balsiger, H., Bar-Nun, A., Berthelier, J.-J., Bieler, A., Bochsler, P., Briois, C., Calmonte, U., Combi, M.R., Cottin, H., De Keyser, J., Dhooghe, F., Fiethe, B., Fuselier, S.A., Gasc, S., Gombosi, I.T., Hansen, C.K., Haessig, M., Jäckel, A., Kopp, E., Korth, A., Le Roy, L., Mall, U., Marty, B., Mousis, O., Owen, T., Rème, H., Rubin, M., Sémon, T., Tzou, C.-Y., Waite, H.J., and Wurz, P. (2016) Prebiotic chemicals—amino acid and phosphorus—in the coma of comet 67P/Churyumov-Gerasimenko. *Sci Adv* 2, doi:10.1126/sciadv.1600285.

Andrade, D.P.P., de Barros, A.L.F., Pilling, S., Domaracka, A., Rothard, H., Boduch, P., and da Silveira, E.F. (2013) Chemical reactions induced in frozen formic acid by heavy ion cosmic rays. *Mon Not R Astron Soc* 430:787–796.

Burgdorf, M., Cruikshank, D.P., Dalle Ore, C.M., Sekiguchi, T., Nakamura, R., Orton, G., Quirico, E., and Schmitt, B. (2010). A tentative identification of HCN ice in Triton. *Astrophys J* 718:L53–L57.

Burton, A.S., Glavin, D.P., Elsila, J.E., Dworkin, J.P., Jenniskens, P., and Yin, Q.-Z. (2014) The amino acid composition of the Sutter's Mill CM2 carbonaceous chondrite. *Meteorit Planet Sci* 49:2074–2086.

Callahan, M.P., Smith, K.E., Cleaves, H.J., Ruzicka, J., Stern, J.C., Glavin, D.P., House, C.H., and Dworkin, J.P. (2011) Carbonaceous meteorites contain a wide range of extraterrestrial nucleobases. *Proc Natl Acad Sci USA* 108:13995–13998.

Cataldo, F., Angelini, G., Hafez, Y., and Iglesias-Groth, S. (2013) Solid state radiolysis of non-proteinaceous amino acids in vacuum: astrochemical implications. *J Radioanal Nucl Chem* 295:1235–1243.

Chakrabarti, S.K., Majumdar, L., Das, A., and Chakrabarti, S. (2015) Search for interstellar adenine. *Astrophys Space Sci* 357:1–10.

Chyba, C. and Sagan, C. (1992) Endogenous production, exogenous delivery and impact-shock synthesis of organic molecules: an inventory for the origins of life. *Nature* 355:125–132.

Cooper, G., Kimmich, N., Belisle, W., Sarinana, J., Brabham, K., and Garrel, L. (2001) Carbonaceous meteorites as a source of sugar-related organic compounds for the early Earth. *Nature* 414:879–883.

Dartois, E., Ding, J.J., de Barros, A.L.F., Boduch, P., Brunetto, R., Chabot, M., Domaracka, A., Godard, M., Lv, X.Y., Mejía Guamán, C.F., Pino, T., Rothard, H., da Silveira, E.F., and Thomas, J.C. (2013) Swift heavy ion irradiation of water ice from MeV to GeV energies: approaching true cosmic ray compaction. *Astron Astrophys* 557:A97–A104.

de Barros, A.L.F., Domaracka, A., Andrade, D.P.P., Boduch, P., Rothard, H., and da Silveira, E.F. (2011) Radiolysis of frozen methanol by heavy cosmic ray and energetic solar particle analogues. *Mon Not R Astron Soc* 418:1363–1374.

de Barros, A.L.F., Boduch, P., Domaracka, A., Rothard, H., and da Silveira, E.F. (2012) Radiolysis of astrophysical ices by heavy ion irradiation: destruction cross section measurement. *J Low Temp Phys* 38:759–765.

de Barros, A.L.F., da Silveira, E.F., Pilling, S., Domaracka, A., Rothard, H., and Boduch, P. (2014) Processing of low carbon content interstellar ice analogues by cosmic rays: implications for the chemistry around oxygen-rich stars. *Mon Not R Astron Soc* 438:2026–2035.

Ehrenfreund, P., Bernstein, M.P., Dworkin, J.P., Sandford, S.A., and Allamandola, L.J. (2001) The photostability of amino acids in space. *Astrophys J* 550:L95–L99.

Evans, N.L., Bennett, C.J., Ullrich, S., and Kaiser, R.I. (2011) On the interaction of adenine with ionizing radiation: mechanistical studies and astrobiological implications. *Astrophys J* 730:69–79.

Fryer, J.R., McConnell, C.H., Zemlin, F., and Dorset, D.L. (1992) Effect of temperature on radiation damage to aromatic organic molecules. *Ultramicroscopy* 40:163–169.

Gerakines, P.A. and Hudson, R.L. (2013) Glycine's radiolytic destruction in ices: first *in situ* laboratory measurements for Mars. *Astrobiology* 13:647–655.

Gerakines, P.A., Moore, M.H., and Hudson, R.L. (2004) Ultraviolet photolysis and proton irradiation of astrophysical ice analogs containing hydrogen cyanide. *Icarus* 170:202–213.

Gerakines, P.A., Hudson, R.L., Moore, M.H., and Bell, J.-L. (2012) *In situ* measurements of the radiation stability of amino acids at 15–140 K. *Icarus* 220:647–659.

Guan, Y.Y., Fray, N., Coll, P., Macari, F., Chaput, D., Raulin, F., and Cottin, H. (2010) UVolution: compared photochemistry of prebiotic organic compounds in low Earth orbit and in the laboratory. *Planet Space Sci* 58:1327–1346.

Günzler, H. and Gremlich, H.-U. (2002) *IR Spectroscopy: An Introduction,* Wiley-VCH, Weinheim.

Hörst, S.M., Yelle, R.V., Buch, A., Carrasco, N., Cernogora, G., Dutuit, O., Quirico, E., Sciamma-O'Brien, E., Smith, M.A., Somogyi, A., Szopa, C., Thissen, R., and Vuitton, V. (2012) Formation of amino acids and nucleotide bases in a Titan atmosphere simulation experiment. *Astrobiology* 12:809–817.

Huang, Q., Su, X., Yao, G., Lu, Y., Ke, Z., Liu, J., Wu, Y., and Yu, Z. (2014) Quantitative assessment of the ion-beam irradiation induced direct damage of nucleic acid bases through FTIR spectroscopy. *Nucl Instrum Methods Phys Res B* 330:47–54.

Hudson, R.L. and Moore, M.H. (2004) Reactions of nitriles in ices relevant to Titan, comets, and the interstellar medium: formation of cyanate ion, ketenimines, and isonitriles. *Icarus* 172:466–478.

Indriolo, N., Geballe, T.R., Oka, T., and McCall, B.J. (2007) $H^{3+}$ in diffuse interstellar clouds: a tracer for the cosmic-ray ionization rate. *Astrophys J* 671:1736–1747.

Krzaczkowska, J., Gierszewski, J., and Ślósarek, G. (2004) Solubility of adenine and kinetin in water–ethanol solutions. *J Solution Chem* 33:395–406.

Loeffler, M.J., Baratta, G.A., Palumbo, M.E., Strazzulla, G., and Baragiola, R.A. (2005) $CO_2$ synthesis in solid CO by Lyman-$\alpha$ photons and 200 keV protons. *Astron Astrophys* 435:587–594.

Martins, Z., Botta, O., Fogel, M.L., Sephton, M.A., Glavin, D.P., Watson, J.S., Dworkin, J.P., Schwartz, A.W., and Ehrenfreund, P. (2008) Extraterrestrial nucleobases in the Murchison meteorite. *Earth Planet Sci Lett* 270:130–136.

Mejía, C., Bender, M., Severin, D., Trautmann, C., Boduch, P., Bordalo, V., Domaracka, A., Lv, X.Y., Martinez, R., and Rothard, H. (2015) Radiolysis and sputtering of carbon dioxide ice induced by swift Ti, Ni, and Xe ions. *Nucl Instrum Methods Phys Res B* 365:477–481.

Mejía, C.F., de Barros, A.L.F., Bordalo, V., da Silveira, E.F., Boduch, P., Domaracka, A., and Rothard, H. (2013) Cosmic ray–ice interaction studied by radiolysis of 15 K methane ice with MeV O, Fe and Zn ions. *Mon Not R Astron Soc* 433:2368–2379.

Mohamed, T.A., Shabaan, I.A., Zoghaib, W.M., Husband, J., Farag, R.S., and Alajhaz, A.E.-N.M.A. (2009) Tautomerism, normal coordinate analysis, vibrational assignments, calculated IR, Raman and NMR spectra of adenine. *J Mol Struct* 938:263–276.

Moore, M., Hudson, R., and Gerakines, P. (2001) Mid- and far-infrared spectroscopic studies of the influence of temperature, ultraviolet photolysis and ion irradiation on cosmic-type ices. *Spectrochim Acta A Mol Biomol Spectrosc* 57:843–858.

Moore, M.H. and Hudson, R.L. (2003) Infrared study of ion-irradiated $N_2$-dominated ices relevant to Triton and Pluto: formation of HCN and HNC. *Icarus* 161:486–500.

Muñoz Caro, G.M. and Schutte, W.A. (2003) UV-photoprocessing of interstellar ice analogs: new infrared spectroscopic results. *Astron Astrophys* 412:121–132.

Nuevo, M., Chen, Y.-J., Hu, W.-J., Qiu, J.-M., Wu, S.-R., Fung, H.-S., Chu, C.-C., Yih, T.-S., Ip, W.-H., and Wu, C.-Y.R. (2014) Irradiation of pyrimidine in pure $H_2O$ ice with high-energy ultraviolet photons. *Astrobiology* 14:119–131.

Oró, J. (1961) Comets and the formation of biochemical compounds on the primitive Earth. *Nature* 190:389–390.

Padovani, M. and Galli, D. (2013) Cosmic-ray propagation in molecular clouds. In *Cosmic Rays in Star-Forming Environments,* edited by D.F. Torres and O. Reimer, Springer, Berlin, pp 61–82.

Palumbo, M.E., Baratta, G.A., Fulvio, D., Garozzo, M., Gomis, O., Leto, G., Spinella, F., and Strazzulla, G. (2008) Ion irradiation of astrophysical ices. *J Phys Conf Ser* 101, doi:10.1088/1742-6596/101/1/012002.

Peeters, Z., Botta, O., Charnley, S.B., Ruiterkamp, R., and Ehrenfreund, P. (2003). The astrobiology of nucleobases. *Astrophys J* 593:L129–L132.

Pilling, S., Andrade, D.P.P., do Nascimento, E.M., Marinho, R.R.T., Boechat-Roberty, H.M., de Coutinho, L.H., de Souza, G.G.B., de Castilho, R.B., Cavasso-Filho, R.L., Lago, A.F., and de Brito, A.N. (2011) Photostability of gas- and solid-phase biomolecules within dense molecular clouds due to soft X-rays. *Mon Not R Astron Soc* 411:2214–2222.

Pilling, S., Andrade, D.P.P., da Silveira, E.F., Rothard, H., Domaracka, A., and Boduch, P. (2012) Formation of unsaturated hydrocarbons in interstellar ice analogues by cosmic rays: unsaturation induced by cosmic rays. *Mon Not R Astron Soc* 423:2209–2221.

Poch, O., Kaci, S., Stalport, F., Szopa, C., and Coll, P. (2014) Laboratory insights into the chemical and kinetic evolution of several organic molecules under simulated Mars surface UV radiation conditions. *Icarus* 242:50–63.

Portugal, W., Pilling, S., Boduch, P., Rothard, H., and Andrade, D.P.P. (2014) Radiolysis of amino acids by heavy and energetic cosmic ray analogues in simulated space environments: glycine zwitterion form. *Mon Not R Astron Soc* 441:3209–3225.

Pullman, B. and Pullman, A. (1963) *Quantum Biochemistry,* Interscience Publishers, New York.

Saïagh, K., Cloix, M., Fray, N., and Cottin, H. (2014) VUV and mid-UV photoabsorption cross sections of thin films of adenine: application on its photochemistry in the Solar System. *Planet Space Sci* 90:90–99.

Sawyer, L.C., Grubb, D.T., and Meyers, G.F. (2008) *Polymer Microscopy,* Springer, New York.

Seperuelo Duarte, E., Domaracka, A., Boduch, P., Rothard, H., Dartois, E., and da Silveira, E.F. (2010) Laboratory simulation of heavy-ion cosmic-ray interaction with condensed CO. *Astron Astrophys* 512:A71.

Severin, D., Trautmann, C., and Neumann, R. (2008) The M-Branch, a new UNILAC irradiation facility with in-situ analytical techniques for materials research. GSI Scientific Report, GSI, Darmstadt, Germany.

Shen, C.J., Greenberg, J.M., Schutte, W.A., and van Dishoeck, E.F. (2004) Cosmic ray induced explosive chemical desorption in dense clouds. *Astron Astrophys* 415:203–215.

Shimoyama, A., Hagishita, S., and Harada, K. (1990) Search for nucleic acid bases in carbonaceous chondrites from Antarctica. *Geochem J* 24:343–348.

van Broekhuizen, F.A., Groot, I.M.N., Fraser, H.J., van Dishoeck, E.F., and Schlemmer, S. (2006) Infrared spectroscopy of solid CO–$CO_2$ mixtures and layers. *Astron Astrophys* 451:723–731.

Webber, W.R. and Yushak, S.M. (1983) A measurement of the energy spectra and relative abundance of the cosmic-ray H and He isotopes over a broad energy range. *Astrophys J* 275:391–404.

Wright, I.P., Sheridan, S., Barber, S.J., Morgan, G.H., Andrews, D.J., and Morse, A.D. (2015) CHO-bearing organic compounds at the surface of 67P/Churyumov-Gerasimenko revealed by Ptolemy. *Science* 349, doi:10.1126/science.aab0673.

Ziegler, J.F., Ziegler, M.D., and Biersack, J.P. (2012) SRIM. www.srim.com

Address correspondence to:
*Gabriel S. Vignoli Muniz*
*Centre de Recherche sur les Ions, les Matériaux et la Photonique*
*Boulevard Henri Becquerel*
*14070 Caen Cedex 05*
*France*

*E-mail:* gabrivignoli2gmail.com

Submitted 15 February 2016
Accepted 6 October 2016

**Abbreviations Used**

DCs = dense clouds
DISM = diffuse interstellar medium
FTIR = Fourier transform infrared
FWHM = full width at half maximum
ISM = interstellar medium
SRIM = Stopping and Ranges of Ions in Matter

# Appendix

Table A1. Apparent Destruction Cross Sections for Selected Absorption Bands

| $\nu_i$ | *Absorption band ($cm^{-1}$)* | *Vibration* | *Xe Apparent destruction cross section ($\times 10^{-14}$ $cm^2$) $Se = 1.12 \times 10^4$ keV $\mu m^{-1}$* | *Kr Apparent destruction cross section ($\times 10^{-14}$ $cm^2$) $Se = 5.8 \times 10^3$ keV $\mu m^{-1}$* | *Ca Apparent destruction cross section ($\times 10^{-14}$ $cm^2$) $Se = 3.13 \times 10^3$ keV $\mu m^{-1}$* | *C Apparent destruction cross section ($\times 10^{-14}$ $cm^2$) $Se = 1.0 \times 10^3$ keV $\mu m^{-1}$* |
|---|---|---|---|---|---|---|
| $\nu_{26}$ | 724 | C6N1, C2N3–R(6) Breathing | 139 ± 6 | 62 ± 2 | 24 ± 2 | 8.9 ± 0.5 |
| $\nu_{25}$ | 797* | C6N10–R(6)–Wagging | 75 ± 6 | — | 30 ± 2 | 6.6 ± 0.3 |
| $\nu_{24}$ | 848 | C8H–R(5)–Wagging | 150 ± 50 | 150 ± 10 | 45 ± 4 | 11.1 ± 0.5 |
| $\nu_{23}$ | 886 | NCN–R(6)–Deformation | 139 ± 4 | 130 ± 3 | 43 ± 1 | 10.1 ± 0.6 |
| $\nu_{22}$ | 914 | NCN–R(5)–Deformation | 222 ± 3 | 109 ± 2 | 45 ± 1 | 12.4 ± 0.6 |
| $\nu_{21}$ | 940 | C2H–R(6)–Wagging | 132 ± 5 | 57 ± 2 | 21.9 ± 0.6 | 6.13 ± 0.02 |
| $\nu_{20}$ | 1025 | NH2–R(6)–Rock | 101 ± 4 | 47 ± 9 | 19 ± 2 | 5.6 ± 0.4 |
| $\nu_{18}$ | 1128 | CN–R(5)–Stretch | 148 ± 7 | 75 ± 2 | 29 ± 2 | 8.0 ± 0.6 |
| * | 1162 | | 182 ± 7 | 100 ± 4 | 56 ± 4 | 15 ± 2 |
| $\nu_{17}$, $\nu_{16}$ | 1255 | C8H–in-plane deformation CN–R(5)–Stretch | 84 ± 4 | 37.2 ± 0.8 | 8.4 ± 0.4 | 4.4 ± 0.1 |
| $\nu_{15}$ | 1309 | CN–R(6)–Stretch | 135 ± 7 | 49.4 ± 0.3 | 24.5 ± 0.9 | 7.3 ± 0.1 |
| $\nu_{14}$ | 1335 | CN–R(5)–Stretch | 116 ± 7 | 64.6 ± 0.5 | 25 ± 1 | 8.5 ± 0.2 |
| $\nu_{13}$ | 1369 | C6N10–Stretch | 190 ± 10 | 99 ± 1 | 51 ± 1 | 14 ± 1 |
| $\nu_{12}$ | 1420 | C2H–in-plane deformation | 98 ± 5 | 33 ± 1 | 24.6 ± 0.5 | 6.4 ± 0.2 |
| $\nu_{11}$ | 1457 | CC–R(6)–Stretch | 270 ± 20 | 8 | — | 9.6 ± 0.9 |
| $\nu_9$ | 1503 | CN–R(5)–Stretch | 96 ± 3 | — | — | IR absorbtion intensity too weak |
| $\nu_8$, $\nu_7$ | 1605 | CN–R(6)–Stretch CC–R(6)–Stretch | 114 ± 5 | 32 ± 1 | 6.5 ± 0.2 | 8.7 ± 0.3 |
| | Part of alpha band** | | 141.9 ± 0.7 | 73 ± 4 | 28.3 ± 0.3 | 6.1 ± 0.1 |
| | Average | | 140.7 | 78.5 | 31.0 | 8.7 |

*To avoid a contribution of a new arising band at 800 $cm^{-1}$, just half the peak area at 797 $cm^{-1}$ was taken into consideration.
**To avoid contribution of water ice absorption, just part of the alpha band was taken into account (2880–2375 $cm^{-1}$).